PROCEEDINGS OF SCIENCE

Development of Affordable and Compact Muon Tomography Detector

Shih-Chieh Su,* **Ying-Chih Chen, Jiwoo Nam, Pisin Chen, and Chung-Yun Kuo**

[a] *Department of Physics and Leung Center for Cosmology and Particle Astrophysics, National Taiwan University, No. 1, Sec. 4, Roosevelt Rd., Taipei 10617, Taiwan*

E-mail: jackysu822@gmail.com

Geiger–Müller Muon Telescope in Taiwan (GMT^2) is an education program for undergraduate students to develop a muon tomography detector composed of Geiger-Müller (GM) tubes. GMT^2 consists of two identical detector plates aligned on an axis at a distance. Each detector plate contains two orthogonal 1-D arrays of 8 GM tubes (L= 18 cm, ø= 2.2 cm), forming an 8×8 grid. The arrival direction of muons can be reconstructed by extrapolating the impact points recorded on two detector plates. Field of view (FOV) of GMT^2 is adjustable by varying the distance between two detector plates. Small size and low unit price of GM tubes make GMT^2 affordable (US\$700) and compact ($40\times40\times40$ cm^3). Several muon tomography experiments were successfully carried out for buildings, such as C.C. Leung Cosmology Hall, National Taiwan University and Taipei 101. In this paper, we report details of system design, detector construction, data acquisition, data analysis, and results.

38th International Cosmic Ray Conference (ICRC 2023)
July 26th – Aug 3rd, 2023
Nagoya, Japan

*Speaker

© Copyright owned by the author(s) under the terms of the Creative Commons Attribution-NonCommercial-NoDerivatives 4.0 International License (CC BY-NC-ND 4.0).

PoS(ICRC2023)531

1. Introduction

Muon tomography is an emerging technique that generates 2-D or 3-D density maps of dense objects utilizing excellent penetrating power and abundant flux of cosmic muons. In recent years, several successful experiments have demonstrated the potential of muon tomography in investigating hidden large structures, including the discovery of a hidden chamber within the Khufu pyramid [1] and the identification of lava chambers within the Guadeloupe volcano [2].

Muon tomography is also an intriguing educational subject for educational due to its intuitiveness and simplicity of the method. Results obtained with the internal density distribution of the objects can be highly visualized, providing a compelling incentive and commanding students' keen interest. In this paper, we report a development of an educational muon tomography detector using Geiger-Müller (GM) tubes. The main considerations in detector design are as follows: 1) The system should be simple enough for undergraduate students to build it themselves. 2) It should be compact, portable, and automotive, allowing for easy experimentation in various locations. 3) The manufacturing cost should be affordable, enabling the project to be carried out within the educational budget of schools. 4) The time required for detector fabrication and experimentation should range from a few months to within one year, ensuring completion within an academic year. This program enables student participation in every aspect of the experimental process, including detector design, fabrication, data taking, data analysis, and simulation.

Our muon tomography detector, named as Geiger Müller muon Telescope in Taiwan (GMT^2), consists of two detection plates, providing a pair of x-y impact points per muon. By extrapolating these paired points, we determine the arrival direction of the incoming muon. The distance between the detection plates is adjustable, providing the flexibility to adjust the field of view (FOV) according to the target being observed. Each detection plate consists of two layers of GM tube arrays, with eight GM tubes arranged in parallel in each layer. By placing these two layers orthogonally to each other, we have implemented an 8x8 x-y grid for obtaining impact point. Using GM tubes, which have a simple and stable operation and are cost-effective, to implement this muon tomography detector meets our requirements exceptionally well. Using commercial GM tubes measuring 22mm in diameter and 180mm in length, we have implemented a 180mm $\times$ 180mm detection plate. With a distance of 200 mm between the two detection plates, a FOV of $90° \times 90°$ is achieved. While it is a drawback that this method does not work for multi-muon events, the probability of multi-muon occurrences within the size of our detector is not significantly high. Designing a high-voltage power supply capable of driving a total of 32 GM tubes, each operating at 400V, presented one of the most formidable challenges in our project. To overcome this, we engineered a cost-effective high voltage supply by leveraging cold cathode fluorescent lamp (CCFL) inverters with a rectifier circuit.

In the following sections, we present a detailed design of the GMT^2 and experimental results for two observation objects to demonstrate the feasibility of our approach.

2. Instrument Design

2.1 High voltage supply

To supply the necessary high voltage for driving the GM tubes, a CCFL inverter is employed. This CCFL inverter, in conjunction with a rectifier circuit, converts the 5V power from the USB

PoS(ICRC2023)531

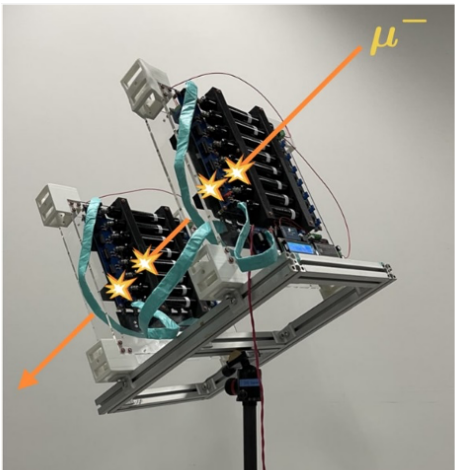

Figure 1: GMT^2 detector

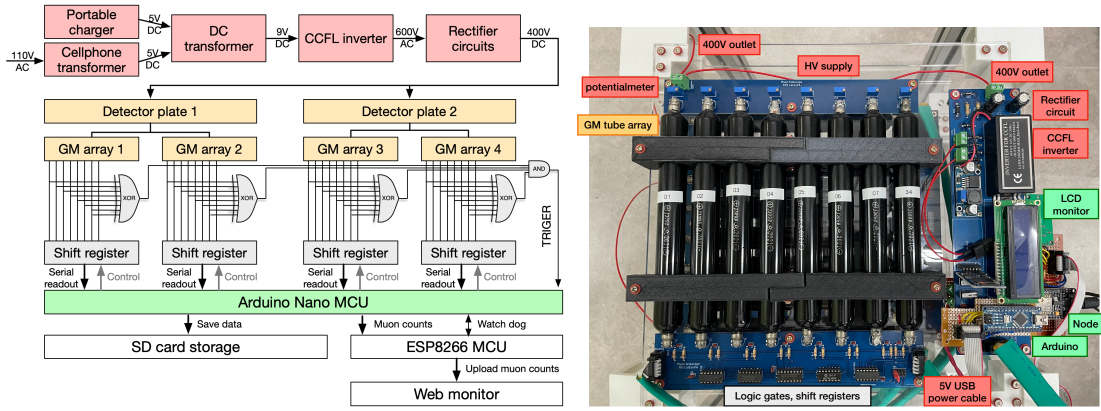

Figure 2: (Left) System schematic diagram. Power module is colored in red, GM tubes are colored in orange, ICs are colored in grey and Data acquisition modules are colored in green. (Right) First layer of GMT^2. The power rectification circuit and MCUs are integrated in a PCB located on first layer. GM tube array is hold by a HV supply board and a signal processing board on each layer.

port to the required working voltage of 400V for the GM tubes. The implementation of the CCFL inverter offers a cost-effective and compact solution for high voltage supply. Additionally, the rectifier circuit ensures a stable power supply, enabling the operation of 32 GM tubes in parallel.

Despite the high voltage requirement, the GM tubes operate at a relatively low current during the electron avalanche process, typically below 10 mA. This results in a total power consumption of only 1.5 Watts. With the advantage of the 5V USB power input, the GMT^2 system becomes portable and self-contained, making it suitable for operation in remote areas using portable chargers.

2.2 Triggers

When particles are detected by the GM tubes, the analog pulse signals undergo an initial digitization process, converting them into square waves using inverters. These digitized signals are then directed to shift registers. Simultaneously, the signals in each layer are fed into XOR gates, ensuring that only one tube within a layer has a signal and rejecting any double hits. The

PoS(ICRC2023)531

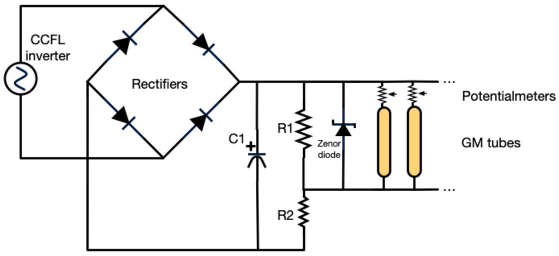

Figure 3: A circuit schematic diagram for the HV module.

PoS(ICRC2023)531

XOR outputs from each layer are subsequently routed to an AND gate, allowing for multi-layer coincidence. This multi-layer coincidence triggers the Arduino MCU, which reads the data from the shift registers. This approach enables the rapid filtering of events that cannot be reconstructed, including electron events.

Pulses from the GM tubes have a pulse width of around 300 ms, introducing a dead time. However, due to the device's low effective area, the likelihood of a second pulse occurring during this dead time is minimal.

2.3 Data acquisition

Once triggered, Arduino reads and processes the data from the shift registers. Although a multi-layer coincidence method is employed, approximately 10% of the events exhibit double hits within the same layer, possibly due to potential cross-talk effects during transmission over a distance of 1 meter. These events are filtered out at this stage, and the remaining events that can be accurately reconstructed are saved to an SD card.

To ensure long-term experimentation, a web monitor and watch dog system are implemented using an additional MCU. This MCU provides Wi-Fi accessibility and monitors the Arduino, calculating the muon counts per minute and uploading the data to the web monitor. In the event of any device malfunctions in the Arduino, it is automatically restarted by the MCU.

3. Experiments

3.1 Chee-Chun Leung Cosmology Hall (CCLCH) experiment

The first muon tomography experiment was conducted in the CCLCH building, which is where our research center is located. The building features a large cylindrical hollow with a diameter of 12 meters and spans across eight floors. Its symmetrical structure along the North-South and East-West axes makes it an ideal subject for verifying the feasibility of GMT^2. Our objective is to observe the inner structure of the CCLCH building.

To achieve this, we performed an exposure to muons that passed through the CCLCH building. This was carried out at the B1 auditorium, with GMT^2 positioned at the center of the building and oriented towards the zenith. Then, we conducted observation of the background muon flux towards the zenith on the rooftop of the CCLCH building (refer to Figure 4(L)). We collected a total of 16 days of data for the attenuated muon flux and 25 days of data for the background muon flux.

3.2 Taipei 101 experiment

Taipei 101, a skyscraper in Taipei that once held the title of the world's tallest building, has been selected as the next target for muon tomography imaging. The objective is to capture the outline of Taipei 101 in the resulting image. After considering various candidates, Xinyi Elementary School was chosen as the experimental site due to its ideal viewing angle and close proximity to Taipei 101.

At Xinyi Elementary School, GMT^2 was positioned in an empty classroom, facing Taipei 101 at N45°E with elevation angle of 45°, allowing for maximum muon penetration. Data collection took place over approximately three weeks for two different field of view (FOV) settings: 90° and 66°. Later, GMT^2 was relocated to an empty classroom at CCLCH while maintaining the same orientation as before, in order to capture the background muon flux from the open sky (refer to Figure 4(R)). The data collection period was extended to 95 days for the 90° FOV and 132 days for the 66° FOV to ensure images with reduced statistical error.

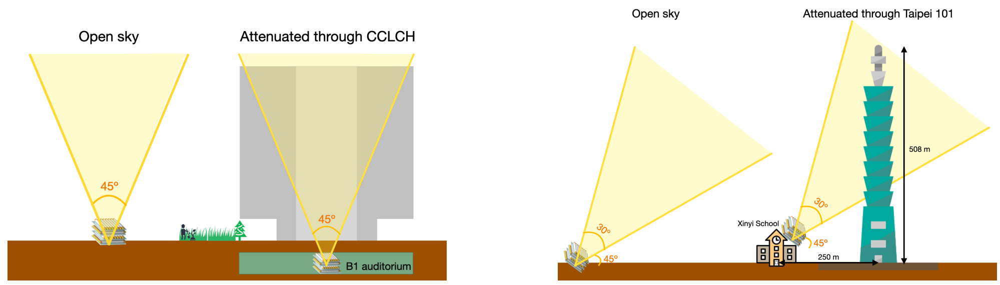

Figure 4: Schematic diagram of apparatus setup for (Left) CCLCH; (Right) Taipei 101 muon tomography image exposure.

3.3 Data analysis

To measure material depth along the muon trajectory, we employ the absorption method. The attenuated muon flux is denoted as $F_i(\theta, \varphi)$, and the background muon flux is denoted as $F_f(\theta, \varphi)$, where (θ, φ) represents the zenith and the azimuth of incoming angle.

The survival rate of muons, given by F_f/F_i, provides information about the interaction depth. By Equation 1, we can determine the corresponding interaction depth for a specific incoming direction.

$$\frac{F_f(\theta, \varphi)}{F_i(\theta, \varphi)} = \exp\left(\frac{\rho \cdot d}{\lambda}\right), \tag{1}$$

where λ is the muon attenuation depth, $1030\,\mathrm{g/cm^2}$ [3] for 4 GeV muons [4] reaching sea-level, density of the material ρ is $2.4\,\mathrm{g/cm^3}$ [5] for concrete in our research, and d is the thickness at a given angle.

The obtained depth is then converted into the thickness of the object, under the assumption that we have prior knowledge of the material's density. In this study, we calculated the ratio between the attenuated muon flux that has passed through the buildings and the muon flux from the open sky, and further transformed it into effective concrete lengths. These lengths correspond to the 2-D density distribution map of the objects and are visualized in our muon tomography images.

PoS(ICRC2023)531

3.4 Simulation

We utilized the Cern ROOT program to construct models of the buildings we observed, namely CCLCH and Taipei 101, and GMT^2 system was placed at the observation location, aligning it with the same orientation as in the actual experiments. In the modeling process, we focused on representing the RC (Reinforced Concrete) framework of the buildings, referring to engineering drawings[5]. To simplify the model, we did not include other structures or materials.

In the simulation program, we generated one million muon rays with random positions and incoming directions. For the muon rays that reached the GMT^2, material lengths along muon trajectories are calculated, and are recorded in the corresponding bin of the expected muon tomography image for the given incoming direction.

This simulation allowed us to generate expected muon tomography images for the observed buildings. By comparing these simulation results with the data collected during the actual experiments, we can verify the feasibility of GMT^2 and assess the level of error present in such long-term observations.

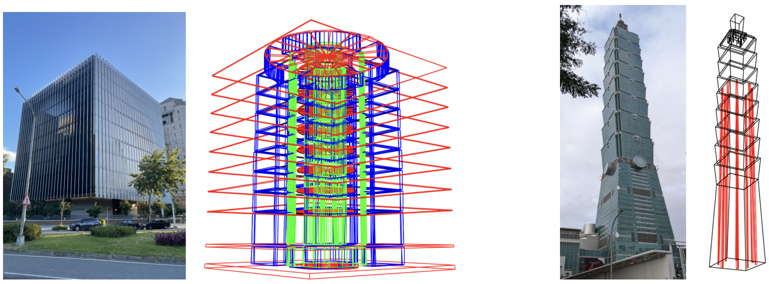

Figure 5: (Left) A model of CCLCH with photo took at same viewing angle. Structural walls around 4 corners are shown in blue and green color, and the cylindrical hollow at the central is shown in red. (Right) A model of Taipei 101 building with photo took at same viewing angle. Taipei 101 building, imitating the segmented structure of bamboo, features eight identical nodes from 26F to 90F, with each node consisting of 8 floors. Eight large pillars colored in red, measuring $3 \times 2\text{m}^2$, support the building from B23F to 90F, with concrete filling below 62F.

4. Results

4.1 Muon tomography image of CCLCH

Muon tomography image along with attenuated and background muon flux historgram are shown in Fig. 6. Total 181k attenuated muons and 529k background muons were collected during 41 days of observation period. The cosine-square distribution due to atmosphere slant depth as well as the effect of larger effective areas at the central due to geometry of GMT^2 could be seen in the central bins of background muon flux histogram(Fig. 6(b)), where much more counts are recorded.

From the muon tomography image (Fig. 6(c)), the cylindrical hollow in CCLCH could immediately be found at the central 9 pixels. Four corners around the hollow has the highest effective length whereas eight bins between them have less concrete, which correspond to the structural walls at four corners of the building and the aisles between the walls. The effective concrete lengths are calculated within a 10% length error for the central 5×5 pixels, which closely

PoS(ICRC2023)531

match with the simulation results. However, there is a larger discrepancy in the outer ring due to lower statistics. This remarkable image captured by GMT^2 has further motivated us to explore our next target object.

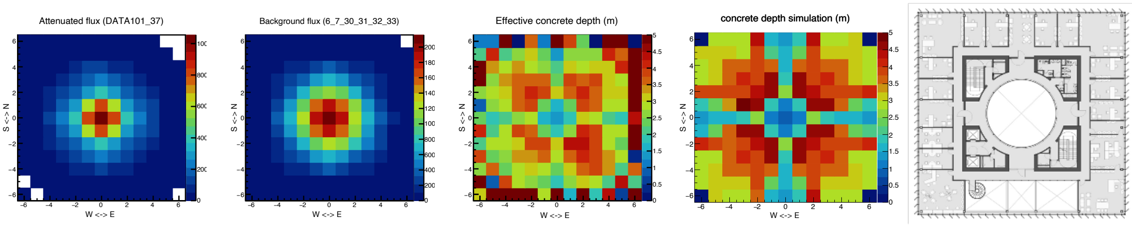

Figure 6: (a) Attenuated muon flux histogram collected in B1F auditorium of CCLCH. (b) Background Muon flux histogram collected at roof top of CCLCH. (c) Muon tomography images showing effective concrete length measured by GMT^2. (d) Expected moun tomography image from simulation. (e) Engineering drawing of 6F of CCLCH building to compare. Position of four structural walls correspond to the thickest concrete length in muon tomography images.

4.2 Muon tomography image of Taipei 101

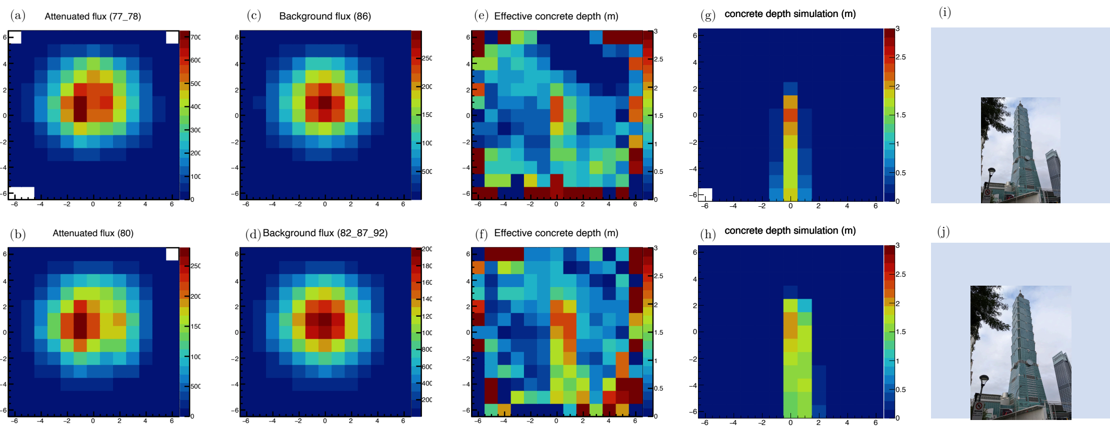

Figure 7: (Row 1) FOV of 90°. (Row 2) FOV of 66°. (Column 1) Attenuated muon flux observed at XinYi Elementary School. (Column 2) Background muon flux observed at an empty classroom in CCLCH. (Column 3) Muon tomography images showing effective concrete length measured by GMT^2. (Column 4) Expected moun tomography images from simulation. (Column 5) Photographic image filmed at Xinyi Elementary School with same orientation of GMT^2.

The muon tomography images of Taipei 101, obtained using different field of view (FOV) settings and compared with simulation results, along with photographic images, are presented in Figure 7. Over a period of 6 weeks at XinYi School, approximately 200k and 9k muons attenuated by Taipei 101 were collected for the two FOV settings. In CCLCH, observations for the background muon flux were conducted for approximately 3 months for each FOV, resulting in a total collection of 732k and 535k background muons for FOV=90° and 66°, respectively.

As seen in Figure 7(e) and 7(f), the muon tomography images reveal a thinner profile of Taipei 101 at the central column for the 90° FOV and the central two columns for the 66° FOV,

PoS(ICRC2023)531

demonstrating the zooming capability of GMT^2. The effective concrete lengths for the central 2×5 pixels of Taipei 101 in the 90° FOV and the central 2×6 pixels in the 66° FOV are calculated with a maximum length error of 10%. In the upper section of Taipei 101, concrete length are larger due to the greater slant depth as muons pass through the building. However, these values gradually decrease for higher floors due to the smaller floor area from the 90th floor. While the comparison of these values with the simulation results is feasible, it should be noted that the simplified Taipei 101 model used in the simulation, which only includes concrete material, may not accurately represent the complexities of the actual building. The inclusion of steel plates, other concrete compartments, and other objects in the simulation is necessary for a more comprehensive analysis.

5. Conclusion and prospects

Muon tomography images of both CCLCH and Taipei 101 building shows the ability of GMT^2 to conduct muon tomography. The effective concrete length is comparable to simulation results, which further demonstrates the feasibility of GMT^2 to reconstruct length of certain material within the FOV. GMT^2 has the ability to capture 14 muon counts per minute for the zenith incoming direction within such a compact device size, and allows us to have 10% error of length estimation under observation period of 1.5 months.

As an educational program for undergraduate students, GMT^2 provides a valuable opportunity to develop essential skills in PCB board design, signal processing, data analysis, and the physics principles underlying this field. The simplicity of operation and the straightforward physical interpretations of the results make the experience highly rewarding. In conclusion, we recommend the implementation of similar educational programs for undergraduate students interested in experimental astrophysics, as it allows them to gain a comprehensive understanding of particle astrophysics.

References

[1] Procureur, S., Morishima, K., Kuno, M. et al., Nat Commun 14, 1144 (2023).

[2] Nolwenn Lesparre et al., Geophys. J. Int. (2012) 190, 1008–1019

[3] S. Cecchini and M. Spurio, arXiv:1208.1171

[4] J.L. Autran, D. Munteanu, T. Saad Saoud, S. Moindjie. Volume 903, 21 September 2018, Pages 77-84

[5] https://www.abri.gov.tw/News_Content_Table.aspx?n=807&sms=9489&s=37438

PoS(ICRC2023)531